Observed Dependence of Stimulated Raman Scattering on Ion-Acoustic Damping in Hohlraum Plasmas

Juan C. Fernández,[1] J. A. Cobble,[1] Bruce H. Failor,[3] Donald F. DuBois,[1] David S. Montgomery,[2,*] Harvey A. Rose,[1] Hoanh X. Vu,[1] Bernhard H. Wilde,[1] Mark D. Wilke,[1] and Robert E. Chrien[1]

[1]*Los Alamos National Laboratory, Los Alamos, New Mexico 87545*

[2]*Lawrence Livermore National Laboratory, Livermore, California 94550*

[3]*Physics International, San Leandro, California*

(Received 25 April 1996)

The reflectivity of a laser due to stimulated Raman scattering (SRS) from long scale-length hohlraum plasmas is shown to depend on the damping of ion-acoustic waves. This dependence is observed in plasmas with either low or high ionization states. Since the SRS process itself is unrelated to acoustic waves, these data are evidence of a nonlinear coupling of SRS to other parametric processes involving daughter acoustic waves. [S0031-9007(96)01182-9]

PACS numbers: 52.35.Mw, 52.40.Nk, 52.50.Jm

Control of laser-plasma instability is important for the success of laser fusion [1], particularly indirect drive [2]. For indirect drive, laser beams enter a cavity (called a hohlraum) made of a material of high atomic number which reaches a high ionization state Z. The high-Z plasma converts laser energy efficiently into x rays, which in turn drive the implosion of a fusion capsule. Because of a relatively long laser-pulse duration, ignition hohlraums, such as those planned for the National Ignition Facility (NIF) [2], are expected to contain underdense plasmas (size $\sim$ few mm) with electron temperatures (T_e) in the keV range. Present NIF-hohlraum designs rely on the plasma pressure from a He-H gas fill to tamp the intrusion into the hohlraum volume by the Au-wall plasma while allowing laser propagation inside the hohlraum [3]. Both in the low-Z fill plasmas and in the high-Z wall plasmas, stimulated Raman scattering (SRS) [4] could be significant.

SRS, the decay of laser light into electron plasma (or Langmuir) waves (LWs) and scattered light [4], has been observed [5] and extensively studied in laser-produced plasmas [6,7]. SRS is undesirable not only because it causes losses in driver energy and target illumination symmetry, but also because LWs trap and accelerate electrons which could preheat the fusion capsule [8].

A strategy to minimize SRS is to decrease its spatial gain by decreasing the laser wavelength and increasing the damping (ν_e) of the LWs. In the regime of interest, Landau damping by electrons is by far the largest contributor to ν_e, which increases by increasing T_e or decreasing the electron density n_e. This strategy has been tested in gas bags [9] and gas-filled hohlraums [10], which achieve high T_e and long scale lengths, relevant to ignition targets, on the Nova laser [11]. The inability to completely suppress SRS in these targets has provided an incentive to further understand SRS.

SRS can couple to other processes, such as stimulated Brillouin scattering (SBS) [12–15]. Other possible coupling mechanisms arise from further parametric decay of the SRS LWs via two distinct mechanisms. One is the electromagnetic decay instability (EDI), in which the LW decays into an ion-acoustic wave (IAW) and a light wave [16,17]. The other is the Langmuir decay instability (LDI), where the SRS LW further decays into an IAW and another LW [18], as seen experimentally [19]. EDI has a lower threshold than LDI because of the lower damping of the EDI daughter light wave compared to the LDI daughter LW. However, if the thresholds for both instabilities are exceeded, the one with the highest growth rate should dominate, i.e., LDI. EDI has lower growth because it has much larger convective losses from the interaction volume due to the larger phase velocity of the daughter light wave.

If coupling to LDI occurs, one might expect the SRS level to increase up to the point where the SRS LW amplitude reaches the threshold for LDI [20]. More correctly, SRS saturation depends on how LDI itself saturates, likely through the further decay cascade of LDI daughter LWs. This cascade has been studied in the weak-coupling limit, where a finite set of linear LWs are excited [21]. Nonlinear theory coupling SRS with Langmuir turbulence [13] is a further advance. Reference [22] presents further numerical simulations of the nonlinear theory in Ref. [13] and a simplified analytical model which agrees with the simulations. Similar work has been done by others [23]. The results are: (i) the SRS reflectivity depends on the ion-acoustic damping (ν_i) of the LDI IAW, i.e., $R_{\mathrm{SRS}} \propto \nu_i/\omega_i$, where ω_i is the frequency of the IAW; (ii) R_{SRS} depends weakly on ν_e, in contrast to the prediction of $R_{\mathrm{SRS}} \propto \nu_e\nu_i$ in Ref. [20].

In this paper, we present novel experimental evidence that the SRS reflectivity R_{SRS} depends on acoustic damping ν_i, which has been varied in large hohlraum plasmas using both high- and low-Z gas fills. We have also studied the dependence of R_{SRS} on T_e and n_e. In particular, use of high-Z gas fills has allowed access to significantly higher T_e on Nova. The preceding Letter also reports a dependence of R_{SRS} on ν_i in high-Z gas-bag plasmas [24], emphasizing low ν_i and temporal beam smoothing.

 0031-9007/96/77(13)/2702(4)$10.00

The results indicate that high ν_i is undesirable SRS control, contrary to the case for SBS [9,10]. We must ultimately learn how to set ν_i to minimize both instabilities.

The Nova gas-filled hohlraum used in our study, described in Ref. [10], is cylindrically symmetric with a length of 1.6 mm and a diameter of 3.2 mm. All ten laser beams have a wavelength of 351 nm. They are arranged in two sets to define two 50° cones with opposing tips along the symmetry axis. All beams enter the hohlraum through one of two laser-entrance holes (LEHs), crossing the symmetry axis 0.1 mm inside their LEH (i.e., 0.7 mm from the midplane). The path from the LEH to the gold wall is about 2 mm. Nine of the ten $f/4.3$ beams (heater beams) turn on at time 0, reaching approximately 2 TW each in 0.1 ns. Power ramps up to 3 TW at time 1.4 ns, when all beams are turned off. An interaction beam is turned on at 0.4 ns and kept at constant power for 1 ns.

Various hohlraum gas fills have been used to study SRS, all at 1 atm pressure and all designed to ionize to $n_e/n_c = 0.11$, where n_c is the critical density above which the laser light cannot propagate. The low-Z gas fills are C_5H_{12}, C_5D_{12}, and CF_4. An illustration of the hohlraum, along with the calculated spatial profiles of n_e, T_e, and T_i for C_5H_{12} are shown in Fig. 1 of Ref. [10]. For C_5H_{12}, $T_e = 3$ keV has been measured [10], in agreement with radiation hydrodynamic simulations using the LASNEX code [25]. To maintain the same $T_e = 3$ keV for CF_4, the heater-beam energy is reduced modestly to compensate for the slightly higher Z of CF_4 relative to C_5H_{12}. All three gases are predicted by LASNEX to exhibit very similar plasma conditions and hydrodynamic evolution.

In order to access higher T_e, high-Z gas fills have been used, i.e., Xe, 70% Xe + 30% C_5H_{12}, and 50% Xe + 50% C_5H_{12}. These fills were shot in two groups: high or low heater-beam energy. In the high-energy case, the heater beams are fired at full energy to reach the highest T_e. In the low-energy case, the total laser energy is halved in order to approach the T_e with low Z. Spectroscopic T_e estimates have been obtained by detecting the x rays from the $n = 4$ to $n = 2$ and the $n = 3$ to $n = 2$ atomic Xe transitions with Bragg-diffraction spectrometers mated to time-resolved detectors [26]. These measurements are interpreted with atomic physics calculations done for plasma conditions in the range of interest [27]. Some spatial resolution is obtained by properly selecting the location and shape of the diagnostic holes, and the lines of sight of the detectors. For example, near the LEH we obtain from both transitions $T_e = 4.0 \pm 0.5$ keV for the low-energy case and $T_e = 6 \pm 1$ keV for the high-energy case, consistent with LASNEX modeling.

Plasma conditions during the period when the interaction beam is on are according to LASNEX fairly constant. Electron density gradients increase slightly as the wall slowly encroaches into the hohlraum interior and as the shock generated by the exploding LEH window moves inward. However, T_e and T_i gradients decrease in time.

In order to calculate ν_i [28], the ratio of T_i/T_e is needed. For the period when the interaction beam is on, LASNEX predicts a typical $T_i/T_e \approx 0.2$ in the low-Z plasmas. In the Xe-doped plasmas, LASNEX predicts $T_i \approx T_e$ due to stronger electron-ion coupling. These values are used to calculate ν_i/ω_i in Fig. 1.

We have gained confidence in the T_i/T_e values from LASNEX by testing the T_i prediction for a mixture of $\frac{1}{3}$Xe + $\frac{2}{3}D_2$. Detection of D-D fusion neutrons with a time-of-flight neutron spectrometer [29] allows a sensitive measurement of the highest T_i in the plasma. The observed peak T_i range of 6–9 keV agrees with LASNEX. This is a test of T_i at the time of interest because LASNEX predicts that, with high Z, T_i peaks at the end of the laser pulse, not much later as in low-Z plasmas.

The main uncertainty in ν_i/ω_i is due to variability in the ratio of T_i/T_e both because of time evolution during the interaction pulse, and because of spatial variations within the target. LASNEX indicates a modest T_i/T_e increase monotonically in time. T_i/T_e evolution is the main source of the error bars in ν_i/ω_i in Fig. 1.

The interaction beam for these experiments is focused by an $f/4.3$ lens with a 3 m focal length. Best focus is placed near the hohlraum midplane so that the distance from best focus to both the LEH and the hohlraum wall is about 1 mm along the beam trajectory. The beam is spatially smoothed by one of two random-phase plates [30,31]. They differ in the sizes of their square random-phase elements, namely 3.1 and 5.8 mm. Given the f number, the peak of the average-intensity envelope in vacuum at both the LEH and wall locations decreases from the peak by a factor of 1.6 for the 3.1 mm plate, and by a factor of 2.8 for the 5.8 mm plate. As the interaction beam penetrates the target, inverse-bremsstrahlung absorption occurs and the intensity decreases. The net effect of beam optics and laser absorption at time 1 ns is summarized in Table I for the shots in Fig. 1. The SRS results are insensitive to which phase plate is used.

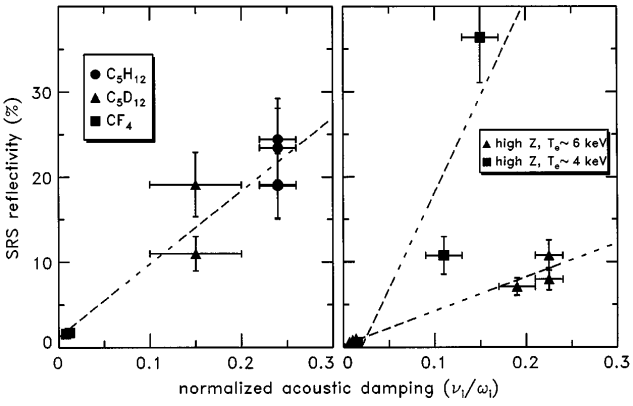

FIG. 1. Raman backscatter reflectivities of the interaction beam are shown for low-Z (left) and high-Z (right) hohlraum gas fills. For high-Z, the high and low-energy cases (labeled by the measured T_e at the LEH) are plotted with different symbols. Least-squares linear fits for all three cases are drawn.

TABLE I. Relative laser intensity at three target locations considering beam optics and calculated laser absorption.

Plasma	RPP	LEH	Midplane	Wall
high Z	3.1 mm	1	0.75	< 0.1
low Z	5.8 mm	1	2.10	0.4
low$Z$	3.1 mm	1	1.20	0.4

Stimulated Raman and Brillouin backscattering are detected with the full aperture backscatter diagnostic (FABS). FABS is capable of SRS and SBS calorimetry, time-resolved spectrometry, and near-field imaging of the scattered light. SRS light outside the beam cone is measured to be negligible.

The backscatter Raman spectra provide information which generally agrees with the calculated plasma conditions in this study. In Fig. 2 we show the time-dependent streaked SRS spectrum detected by FABS from a hohlraum initially containing 0.97 atm of 50% Xe + 50% C_5H_{12} gas, illuminated with a total laser energy of 30.7 kJ. The time-average spectrum peaks at 580 nm, which is consistent with $n_e/n_c = 0.1$ at $T_e = 5$ keV, the expected volume-average n_e. Shot to shot variations of up to $\pm 10\%$ in the peak wavelength can occur.

In Fig. 2 the SRS power increases in time, a general trend in our data. In keeping with our main result, we attribute this SRS increase to an increase of ν_i/ω_i in time corresponding to the predicted increase in T_i/T_e.

The time-integrated SRS reflectivity data are shown in Fig. 1. The three data sets in this figure clearly show that as acoustic damping increases, SRS reflectivity increases. Figure 1 (left) verifies the scaling in the case of low Z without the potential complication of high inverse-bremsstrahlung absorption of SRS light originating deep within the plasma. This would complicate the interpretation of our measurements. However, low SRS reflectivities from both CF_4 and Xe (even though inverse-bremsstrahlung absorption is very different) discount absorption of SRS light as the source of the trend. Also, we measure lower reflectivities from the high-Z, high-T_e plasmas than from the high-Z, low-T_e plasmas. This tendency is opposite to that one would expect from strong absorption of SRS light from deep within the hohlraum.

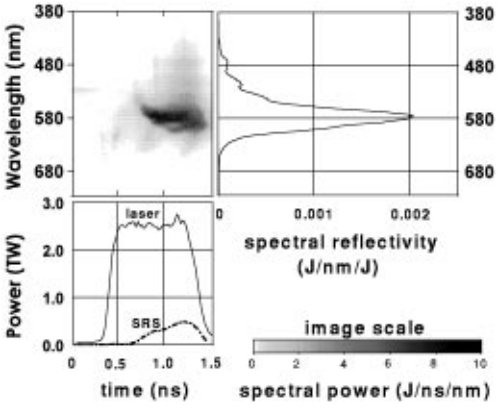

FIG. 2. The Raman backscatter spectrum is shown for shot 25102319. SRS time-integrated reflectivity is 11%. Plots of the interaction beam and reflected SRS powers (bottom) and of the time-integrated spectrum (right) are shown.

The data in Fig. 1 demonstrate that the dependence of the SRS reflectivity on acoustic damping is a general effect observed for a wide range of Z and T_e. In Fig. 1, interaction-beam intensities at the LEH are $(2-3.6)\times 10^{15}$ W/cm^2 for low-Z, $(2-2.8)\times 10^{15}$ W/cm^2 for high-Z high-T_e, and $(2.3-2.4)\times 10^{15}$ W/cm^2 for high-Z, low-T_e plasmas. The observed scaling versus ν_i is consistent with the linear scaling predicted from SRS saturation either by Langmuir turbulence [22] or by EDI. High values of ν_e cannot compensate and significantly increase the reflectivity if ν_i is small. Shots with 67% Xe + 33% H_2 (not in Fig. 1), having a volume-averaged $n_e/n_c = 0.08$ but the same T_e, should have a much higher ν_e but the same ν_i as pure Xe. However, with both fills SRS reflectivities are similar (below 1%).

SRS in these hohlraums is apparently saturated rather than in a spatial-gain-limited regime. For example, in other C_5H_{12} shots with higher interaction-beam intensity at the LEH (5×10^{15} W/cm^2), the SRS reflectivities average 22%, the same as with the typical 2.5×10^{15} W/cm^2 in Fig. 1. Thus the dependence of SRS gain on intensity in linear theory is not manifest here.

We discard the possibility that IAWs from SBS are detuning SRS and controlling the observed R_{SRS} scaling with ν_i in our plasmas. For example, for CF_4 relative to C_5D_{12}, the SBS reflectivity is similar ($\approx 10\%$), while the SRS reflectivity is an order of magnitude lower (see Fig. 1). And for C_5H_{12} relative to C_5D_{12}, the SRS reflectivity is modestly higher while the SBS reflectivity is lower by an order of magnitude.

In Fig. 1, the slope of R_{SRS} versus ν_i depends on T_e. In a sufficiently hot plasma, SRS should saturate via EDI, rather than Langmuir turbulence, because LDI, i.e., the necessary first step towards turbulence, is inaccessible. In the strongly damped SRS regime [21] but below the threshold for secondary instabilities, the LW amplitude E_L satisfies $E_L \sim R_{\mathrm{SRS}}^{1/2} I/\nu_e$, where I is the laser intensity. The LDI threshold is $E_L^2 \sim \nu_i \nu_e$ [20]. These relations imply $R_{\mathrm{SRS}} \sim \nu_e^3 \nu_i / I^2$. Because $R_{\mathrm{SRS}} < 1$, it follows that, given ν_i and I, LDI is inaccessible to SRS for sufficiently high T_e and sufficiently low n_e. Well within LDI accessability, Langmuir turbulence can develop, and the dependence of R_{SRS} on ν_e weakens significantly. If R_{SRS} is measured, then that contour (rather than $R_{\mathrm{SRS}} = 1$) demarcates the region of LDI accessibility. Figure 3 shows the $R_{\mathrm{SRS}} = 0.5, 0.05$ contours of LDI accessibility for $\nu_i = 0.01$ and hot spots with $I = 10^{16}$ W/cm^2. Outside LDI accessibility, EDI could also yield $R_{\mathrm{SRS}} \propto \nu_i$ (same dependence on ν_i at the EDI threshold), but SRS levels might be higher. Nonlinear SRS saturation via EDI is being explored in work underway, analogous to that

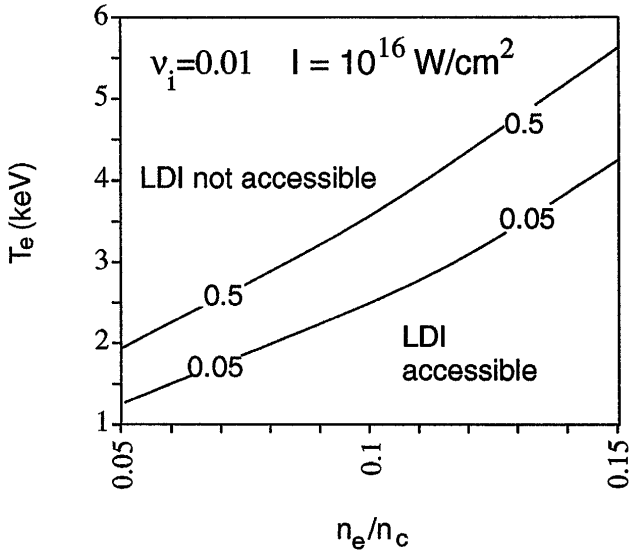

FIG. 3. 50% and 5% reflectivity contours for accessibility of LDI, assuming a Maxwellian electron distribution. The 100% contour is close to the 50% contour shown. Increased ν_i and lower I move the contours modestly towards lower T_e.

done for LDI [22]. Exploring SRS behavior across the LDI boundary seems promising with our low-Z plasmas, which lie near the boundary. LDI accessibility is harder to evaluate in high-Z plasmas, where the higher ZI/T_e is, the more the electron distribution deviates from a Maxwellian [32,33]. In such distributions, ν_e decreases significantly [34], moving the LDI boundary to higher T_e.

In summary, we present novel direct evidence for the dependence on acoustic damping of the SRS reflectivity of a 351 nm RPP laser beam from a long-scale-length hohlraum plasma. Since SRS itself is unrelated to acoustic waves, this is evidence of other parametric processes determining the nonlinear saturation of Raman backscatter. This dependence is observed in plasmas with high and low ionization states for a wide range of electron temperatures and normalized acoustic damping relevant to ignition hohlraums. The observed scaling of SRS versus acoustic damping is consistent with the linear scaling expected from saturation either by Langmuir decay instability and Langmuir turbulence, or by electromagnetic decay instability, in their respective regimes of applicability.

We thank the Nova operations team, the Los Alamos technicians supporting Nova, the target fabrication group at Los Alamos, K. Gifford (GA) and G. Stone (LLNL). J. Miller (LLNL) did the optics design of the FABS diagnostic. A. Osterheld (LLNL) performed theoretical atomic physics calculations relevant to this paper. This work was supported by the U.S. DOE.

*Present address: Los Alamos National Laboratory, Los Alamos, NM 87545.

[1] J. H. Nuckolls, L. Wood, A. R. Thiessen, and G. B. Zimmerman, Nature (London) **239**, 139 (1972).
[2] J. D. Lindl, R. L. McCrory, and E. M. Campbell, Phys. Today **45**, 32 (1992).
[3] S. W. Haan *et al.*, Phys. Plasmas **2**, 2480 (1995).
[4] M. V. Goldman and D. F. DuBois, Phys. Fluids **8**, 1404 (1965).
[5] R. G. Watt, R. D. Brooks, and Z. A. Pietrzyk, Phys. Rev. Lett. **41**, 170 (1978).
[6] R. P. Drake *et al.*, Phys. Fluids **31**, 3130 (1988).
[7] H. A. Baldis, E. M. Campbell, and W. L. Kruer, in *Physics of Laser Plasma*, Handbook of Plasma Physics (North-Holland, Amsterdam, 1991), Vol. 3, Chap. 9, pp. 361–434.
[8] R. P. Drake *et al.*, Phys. Rev. Lett. **53**, 1739 (1984).
[9] B. J. MacGowan *et al.*, Phys. Plasmas **3**, 2029 (1996).
[10] J. C. Fernández *et al.*, Phys. Rev. E **53**, 2747 (1996).
[11] E. M. Campbell, Rev. Sci. Instrum. **57**, 2101 (1986).
[12] C. J. Walsh, D. M. Villeneuve, and H. A. Baldis, Phys. Rev. Lett. **53**, 1445 (1984).
[13] H. A. Rose, D. F. DuBois, and B. Bezzerides, Phys. Rev. Lett. **58**, 2547 (1987).
[14] D. M. Villeneuve, H. A. Baldis, and J. E. Bernard, Phys. Rev. Lett. **59**, 1585 (1987).
[15] H. A. Baldis *et al.*, Phys. Rev. Lett. **62**, 2829 (1989).
[16] V. N. Tsytovich, *Nonlinear Effects in Plasmas* (Plenum, New York, 1970), Chap. 5, p. 127.
[17] K. L. Baker, Ph.D. dissertation, University of California at Davis, 1996.
[18] D. F. DuBois and M. V. Goldman, Phys. Rev. Lett. **14**, 544 (1965).
[19] K. L. Baker *et al.*, Phys. Rev. Lett. **77**, 67 (1996).
[20] R. P. Drake and S. H. Batha, Phys. Fluids B **3**, 2936 (1991).
[21] J. A. Heikkinen and S. J. Karttunen, Phys. Fluids **29**, 1291 (1986).
[22] B. Bezzerides, D. F. DuBois, and H. A. Rose, Phys. Rev. Lett. **70**, 2569 (1993).
[23] T. Kolber, W. Rozmus, and V. T. Tikhonchuk, Phys. Fluids B **5**, 138 (1993).
[24] R. K. Kirkwood *et al.*, following Letter, Phys. Rev. Lett. **77**, 2706 (1996).
[25] G. Zimmerman and W. Kruer, Comments Plasma Phys. Control. Fusion **2**, 51 (1975).
[26] B. H. Failor, R. Hockaday, and W. W. Hsing, Rev. Sci. Instrum. **66**, 767 (1995).
[27] C. J. Keane, B. A. Hammel, A. L. Osterheld, and D. R. Kania, Phys. Rev. Lett. **72**, 3029 (1994).
[28] H. X. Vu, J. M. Wallace, and B. Bezzerides, Phys. Plasmas **1**, 3542 (1994).
[29] R. E. Chrien, D. F. Simmons, and D. L. Holmberg, Rev. Sci. Instrum. **63**, 4886 (1992).
[30] Y. Kato *et al.*, Phys. Rev. Lett. **53**, 1057 (1984).
[31] S. M. Dixit *et al.*, Appl. Opt. **32**, 2543 (1993).
[32] A. B. Langdon, Phys. Rev. Lett. **44**, 575 (1980).
[33] P. Alaterre, J. P. Matte, and N, Lamoreux, Phys. Rev. A **34**, 1578 (1986).
[34] B. B. Afeyan, A. E. Chou, and W. L. Kruer, "Landau Damping of Electron Plasma Waves in Flat Top Distribution Functions" (to be published).